J Fluoresc (2012) 22:875–882
DOI 10.1007/s10895-011-1025-x

ORIGINAL PAPER

Whole-Object Fluorescence Lifetime Setup for Efficient Non-Imaging Quantitative Intracellular Fluorophore Measurements

Yaniv Namer · Lior Turgeman · Mordechai Deutsch · Dror Fixler

Received: 27 September 2011 / Accepted: 21 November 2011 / Published online: 20 January 2012

Abstract In the present study we introduce a Whole-Object Fluorescence Life Time (wo-FLT) measurement approach for ease and a relatively inexpensive method of tracing alterations in intracellular fluorophore distribution and in the physical-chemical features of the microenvironments hosting the fluorophore. Two common fluorophores, Rhodamine 123 and Acridine Orange, were used to stain U937 cells which were incubated, with and without either Carbonyl cyanide 3-chlorphenylhydrazon or the apoptosis inducer H_2O_2. The wo-FLT, which is a non-imaging quantitative measurement, was able to detect several fluorescence decay components and corresponding weights in a single cell resolution. Following cell treatment, both decay time and weight were altered. Results suggest that the prominent factor responsible for these alterations and in some cases to a shift in emission spectrum as well, is the intracellular fluorophore local concentration. In this study it was demonstrated that the proposed wo-FLT method is superior to color fluorescence based imaging in cases where the emission spectrum of a fluorophore remains unchanged during the investigated process. The proposed wo-FLT approach may be of particular importance when direct imaging is impossible.

Y. Namer · M. Deutsch (✉)
The Biophysical Interdisciplinary Jerome Schottenstein Center for the Research and the Technology of the Cellome,
Physics Department, Bar-Ilan University,
Ramat-Gan 52900, Israel
e-mail: rtcellom@mail.biu.ac.il

L. Turgeman · D. Fixler (✉)
Faculty of Engineering and the Institute of Nanotechnology and Advanced Materials, Bar Ilan University,
Ramat Gan 52900, Israel
e-mail: Dror.Fixler@biu.ac.il

Keywords Fluorescence life time · Fluorescence dye concentration · Membrane potential · Whole-object fluorescence life time measurements

Abbreviations

FLT	fluorescence lifetime
wo-FLT	Whole-Object Fluorescence Life Time
FI	Fluorescence intensity
FLIM	Fluorescence life-time imaging
PMP	plasma membrane potential
AO	Acridine Orange
Rh123	Rhodamine 123
CCCP	Carbonyl cyanide 3-chlorophenylhydrazone

Introduction

One of the most powerful tools in cell research is fluorescence based cytometry [1]. Fluorescence is an attractive method of detecting physiological processes in biomedical applications. Fluorescent markers are widely applied to label molecules, cells and tissues [2]. Upon excitation of a fluorescent molecule from its ground electronic state to a higher electronic state, the molecule will reside transiently in its primarily excited electronic state, usually in the range of picoseconds to tens of nanoseconds. The average time the molecule spends in the excited electronic state is referred to as the fluorescence lifetime (FLT). There is an extensive history of FLT measurement experiments (macroscopic samples in cuvettes) [3–5]. However, as fluorescing molecules have different FLTs, time resolved measurements of fluorescence have provided a wealth of invaluable information in general and of biological systems in particular. In the current research we propose to use whole-object FLT (wo-

FLT) as a cellular physical indicator for intracellular biological changes.

Fluorescence intensity (FI) measurement is commonly used in analytical chemistry [6]. This is mainly based on the fact that fluorophore spectroscopic features are extremely sensitive to the chemical-physical nature of their hosting media (e.g. presence of quenchers, of oxygen, pH level, viscosity, polarity, polarizability, etc.) and may be used for estimation of fluorophore concentration as well. In many instances intracellular fluorophores (even of the same type) tend to occupy various sub-cellular regions (organelles), a fact which is, most probably, reflected in the whole stained cell emission.

Sub-cellular compartments may accumulate fluorophores and consequently elevate the latter's local concentration. More specifically, certain fluorophores tend to concentrate at regions where the ionic concentration is high, relative to the surrounding area. This feature is commonly used for the tracing and mapping of variations in plasma membrane potential (PMP) in living and excitable cells, under the assumption that the FI is linearly proportional to the fluorophore concentration [7, 8]. FI is also used for detection of DNA hybridization concentration. Single-molecule Fluorescence measurements of biomolecules can provide information about the molecular interactions and kinetics that are hidden in ensemble measurements. Detection of DNA hybridization at the single-molecule level using such method [9] is an important biotechnology for qualitative and quantitative analysis [10].

However, tracing alterations in fluorophore concentration via FI measurements has some limitations possibly affecting the reliability of FI-based bioassays: FI is an absolute measure-hence sensitive to the instability of excitation light source intensity, electrical noises, etc. and, due to its local chemical-physical features, a given fluorophore may behave differently and even become quenched while in different cellular organelles. Therefore, the quantum yield of the dye may change due to environmental fluctuation and the heterogeneity in FI cannot be unequivocally attributed to local fluorophore concentration.

On the other hand, these variations (in emission/absorption spectra, quenching, etc.) of the same type of molecule are generally associated with corresponding changes in their FLTs. This fact however, might be of significant advantage upon collective common FI measurements, since the first approximation of collective measured FLT may be a linear sum of pure exponential decay components which might be elegantly distinguished and related to their sources [11]. In that respect, a non image, wo-FLT measurement is expected to yield more than a single decay component. Obviously, both FLTs and respected weights might change in the course of cell activation.

In the present study, Acridine Orange (AO) stained U937 cell lines were investigated. FLT measurements were performed on cells treated with and without H_2O_2, which is generally known to induce apoptosis [12, 13], and were specifically tested by us in previous publication [14]. Cellular staining by AO is heterogeneous and its emission was found to have several decay components. However, incubating the cells with H_2O_2 altered the decay components and their weights. This was correlated thereafter, with intracellular changes of AO distribution. Complementary experiments were performed with Rhodamine 123 stained U937 cells that were treated with and without CCCP, which is known to alter PMP [15, 16].

Materials and Methods

Dyes

AO, Rhodamine 123 (Rh123), Hydrogen Peroxide (H_2O_2), Deoxyribonucleic Acid from calf thymus (DNA) and Carbonyl cyanide 3-chlorophenylhydrazone (CCCP), were obtained from Sigma-Aldrich (St.Louis, MO, USA). Rh123 (13 μM), AO (10 μM) and CCCP (50 μM) working solutions were prepared by dissolving them in Phosphate Buffered Saline (PBS) with pH=7.4. Bulk measurements were performed with 10^{-7} M and 10^{-2} M AO solutions. The term "bulk measurement" herein refers to solution measurements using cuvette.

Cell Line

U937 cells were maintained in RPMI-1640 medium supplemented with 10% heat-inactivated fetal calf serum, 100U/mL penicillin, 100 μg/mL streptomycin, 2% glutamine, 2% sodium pyruvate and 2% HEPES (complete medium). All the materials were obtained from Biological Industries (Kibbutz Beit Haemek, Israel). Cells were maintained in completely humidified air with 5% CO_2 at 37 °C. Before use, the exponentially grown cells were collected, washed and re-suspended at a concentration of 2×10^6 cells/mL.

Cell Labeling and Treatment

Rh123: Cells, at a concentration of 2×10^6 cells/mL in PBS, were stained for 30 min at 37 °C, 5% CO_2, with 13 μM Rh123, double washed by centrifugation 1,000 RPMI for 5 min with 5 ml of PBS and re-suspended at a concentration of 2×10^6 cells/mL in PBS.

AO: Cells, at a concentration of 2×10^6 cells/mL in PBS, were stained for 15 min at room temperature, with 10 μM AO.

CCCP Inducer: CCCP was added to cell suspension to a final concentration of 50 μM.

Apoptosis Inducer: Cells were incubated with 50 μM H_2O_2 for a period of 2 h at 37 °C, 5% CO_2. In all cases cell staining was performed after cell treatment.

Measurement System

Bulk Measurements

Bulk FLT measurements were performed by the K-2 Multi-frequency Cross-Correlation Phase and Modulation Fluorimeter (ISS, Illinois, USA). Samples were excited with a 488 nm polarized beam of a CW argon ionic laser model 161B-070 (Spectra-Physics, USA), which was modulated at the frequency range of 1 kHz to 500 MHz. In most experiments, 10 frequencies were used, ranging from 2 MHz to 200 MHz on a logarithmic scale.

Bulk absorption, scattering and fluorescence spectra measurements were performed using a Perkin Elmer spectrofluorimeter, Model MPF-44 (Waltham, Massachusetts USA) and Shimadzu UV-1650PC spectrophotometer (Duisburg, Germany).

Microscopic Measurements

Measurements of FI and FLT of microscopic samples were performed using a Frequency Domain Time-Resolved Microscope (FDTRM) [17]. Schematic depiction of the FDTRM is shown in Fig. 1. The FDTRM comprises two main stand-alone components: the optical system-an upright epi-fluorescent Zeiss microscope Z-1, and a modified frequency domain FLT and FAD ISS K-2 spectrofluorimeter. For FLT measurements, the excitation and emission polarizers of the FDTRM were configured to measure at a set of magic angles [18]. As shown in Fig. 1, the FDTRM may be used for bulk measurement by connecting the PMTs to a cuvette system.

Fluorescence images were acquired using an Olympus IX81 microscope equipped with a PixeLINK PL-A662 10 bit RGB CCD camera (Ontario, Canada) and a 14-bit ORCA II C4742-98 camera (Hamamatsu, Japan).

Fluorescence life-time images (FLIM) were acquired using a Becker & Hickl GmbH (Berlin, Germany) DCS-120 confocal FLIM system [19].

Results

wo-FLT Versus FLIM Measurements of AO Stained U937 Cells

Intracellular AO, in the cytoplasm, usually appears as a monomer [20] which emits green fluorescence with a peak value at 530 nm [21]. However, in some organelles (e.g. lysosomes) AO molecules tend to aggregate to dimmers [22–24], emitting red fluorescence with a peak value at 580 nm [21]. Some studies show that the source for intracellular red fluorescence is lysosomal highly concentrated AO [24, 25]. These two states can be identified in Fig. 2, where color (upper panel) and FLT (lower panel) images of AO stained U937 cells are presented.

The correlation of these results with bulk measurements was examined via two extreme concentrations of AO solutions, 10^{-7} M and 10^{-2} M**.** In order to minimize inner filtration influence in these bulk measurements, excitation and collection of fluorescence were performed from the front face that is on the same side of a triangular cuvette. Bulk measurement results (summarized in Table 1) clearly indicate that the emission peak of 530 nm (green, 10^{-7} M AO) is associated with FLT of 2 nsec and the emission of

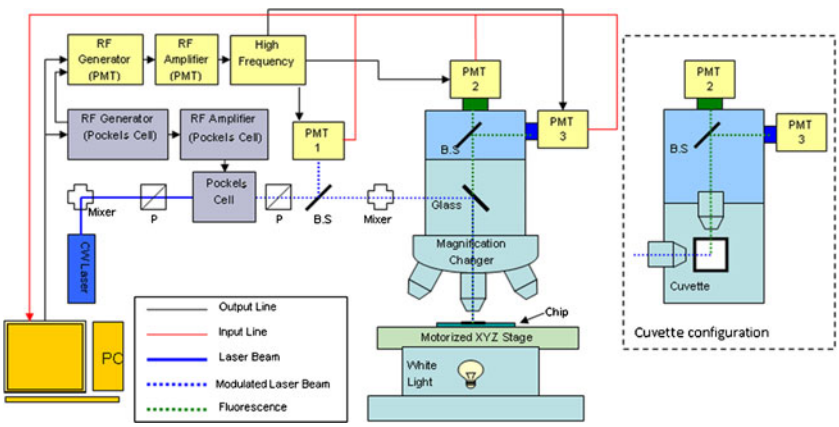

Fig. 1 Schematic representation of the FDTRM apparatus. The laser light passes through the Pockels cell and excites the sample. The Pockels cell and the detectors (PMT) are modulated by two frequency synthesizers and two RF amplifiers. The entire measurement process, including data acquisition and analysis are controlled by a personal computer. Data can be collected by microscope system, as well as bulk measurement system (cuvette configuration). Note: P Polarizer and B.S Beam Splitter

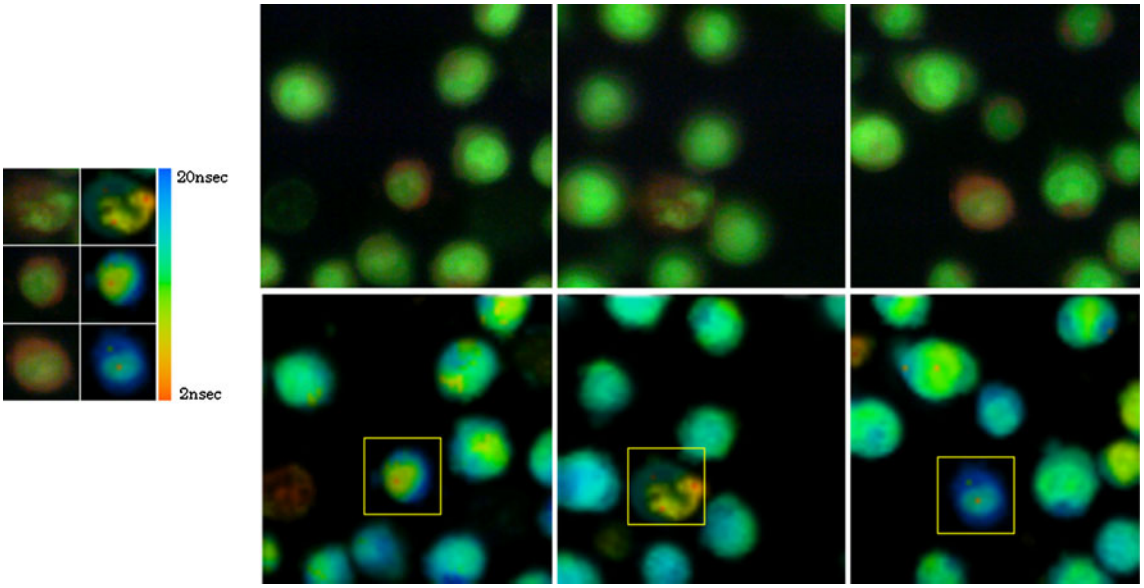

Fig. 2 Fluorescence images of U937 AO stained cells acquired via PixeLINK PL-A662 10 bit color camera (*upper panel*) and via FLIM system of Becker & Hickl DCS-120 system (*lower panel*). FLIM color scale ranges from 2 nsec (*red*) up to 20 nsec (*blue*). To ease comparison between corresponding images, three cells (marked with a yellow square in the lower panel) were chosen and placed in the insert, wherein their direct fluorescence image appears in the left column and their corresponding FLIM in the right column

640 nm (red, 10^{-2} M AO) is associated with an FLT of 20 nsec. These results are in agreement with others [26–28].

The ability of wo-FLT measurement (skipping FLIM) to "blindly" distinguish between said regions, were examined consecutively on 50 cells using the FDTRM system and results are listed in Table 2.

The averaged FLT values (see upper panel of Table 2) indicate a remarkable similarity to those obtained using only solutions (Table 1). This suggests that the long FLT (20 nsec) is most likely attributed to the highly concentrated intracellular AO regions, which correspondingly are shown to have reddish emission (Fig. 2). In addition, wo-FLT measurements indicate that the weight of the emission decay component of these AO high concentrated hosting regions is 30% out of the whole cell emission (Table 2, f_1=0.3).

In a similar manner, one may ascribe the 1.89 nsec decay component to the low density of AO hosting regions, which are most likely to emit yellowish fluorescence, weighing 40% of the whole cell emission. However, the origin of the 6.1 nsec component needs to be explained unrelated to the low and high AO densities.

Table 1 Maximum absorption and emission wavelengths and corresponding FLTs of two AO solutions with 10^{-7} M and 10^{-2} M concentrations as measured in Bulk with Phosphate buffered saline at pH=7.4

	AO 10^{-7} M	AO 10^{-2} M
Maximum Absorption	495 nm	465 nm
Maximum Emission	530 nm	640 nm
Fluorescence Lifetime	2×10^{-9} s	20×10^{-9} s

FLIM of U937 AO Stained Cells

FLIM complementary measurements were performed on the same AO stained cells (Fig. 2, lower panel). FLT values are indicated by color in a single pixel resolution. At least three colored intracellular region colors, each indicating a different life time, are distinguishable: blue, green and red regions indicate FLTs of 19.8±4 nsec, 2.1±0.2 nsec and of 5.45± 0.6 nsec respectively. As a matter of interest, fluorescence gathered from areas between cells, namely that of extracellular AO, show a single decay component of 2.12± 0.09 nsec.

The FLIM results are in high agreement with the results obtained via FI color images (Fig. 2) and via wo-FLT measurements. Comparative examination of Fig. 2 indicates that the deep red regions, which appear in the FI color images, correlate with the long (~20 nsec, orange-red) FLT regions of the FLIM. In addition, FLIM measurement validated that the source of the 2 nsec FLT is the free-flowing AO in PBS, correlating with the FLT of the signal measured within regions in between cells. Unlike the 2 and 20 nsec components which could be distinguished by their emission spectra, the intracellular regions of the 6 and 2 nsec decay component could not be distinguished by their emission. However, the existence of the 6 nsec component measured via wo-FLT was validated by FLIM, as well. Failure of the emission based differentiation approach observed here could

Table 2 FLT values measured in U937 cells stained with AO after incubation with and without 50 μM H_2O_2 for a period of two hours at 37 °C**.** The f is the weight of the decay component while Σf=1. Results are expressed as average of 50 cells ± STD. $P<0.01$

Treatment	τ_1 [nsec]	f_1	τ_2 [nsec]	f_2	τ_3 [nsec]	f_3
Control	23±2.2	0.3±0.02	6.1±0.8	0.32±0.035	1.89±0.23	0.38±0.041
H_2O_2	20	0	6±1.1	0.42±0.08	1.91±0.7	0.58±0.075

be caused by either: (a) low color resolution of the camera used, or (b) similar emission spectra in the two regions, a case which illustrates well where wo-FLT can succeed while the more commonly used spectra based FI image analysis may fail.

It is proposed that the dissimilarity between the FLTs and their related weights is attributed to the difference in the physical-chemical features of the two hosting regions. In an effort to allocate the intracellular source of the 6 nsec fluorescence component, four DNA:AO mixtures were prepared based on previous studies [29, 30]; 0:100, 1:100, 5:100, and of 8.5:100, and their FLTs were measured using our new wo-FLT method. Results clearly indicate that the higher the DNA concentration, the more dominant the 6 nsec component is (Table 3). This strongly suggests that the AO-DNA complex is the source for the 6 nsec decay component measured using wo-FLT and is further strengthened by the fact that the higher the DNA concentration, the lower the weight of the 2 nsec decay component obtained with just AO in PBS.

FLT Measurements of H_2O_2 Treated U937 Cells

The FLT of intracellular AO was measured in U937 cells following their incubation without and with 50 μM H_2O_2 for a period of 2 h at 37 °C. H_2O_2 is known to induce apoptosis [4]. The results are shown in the lower panel of Table 2.

As can be seen in the table, the long FLT component (~20 nsec) ceases to exist, while the two short FLT components remain in relation to that obtained when cells were incubated without (Control) (H_2O_2-Table 2 upper panel). However, after incubation with H_2O_2, the weights of the decay component (f) were altered as well. The 1.91 nsec component increased from 38% to 58%, and that of the 6 nsec-from 32% to 42%.

Table 3 FLT values measured in different DNA:AO ratios. The AO concentration was 10 μM at Phosphate buffered saline with pH=7.4. The f is the weight of the decay component. Results are expressed as average of 20 cells ± STD. P<0.001

DNA:AO	Lifetime	
	f	τ_F [nsec]
0:100	1	1.89±0.1
1:100	0.195±0.05	6.2±1.2
	0.805±0.1	1.89±0.1
5:100	0.328±0.11	6.3±2.1
	0.672±0.23	2±0.25
8.5:100	1	6±1.3

Measuring FLT from U937 Cells Stained with Rhodamine 123

FLT of Rh123, in the presence and absence of CCCP, has been used to trace membrane potential. CCCP acts as a weak lipophilic acid that penetrates the cell membrane, binds to H^+ proteins outside the mitochondria and then enters the mitochondria matrix and releases the proteins. Thus, H^+ protein gradient ceases to exist across the mitochondria membrane [15, 16].

Measurements of wo-FLT were conducted on 30 individual cells following incubation without and with CCCP, using the FDTRM system. Cells were stained with 13 μM Rh123. FLT, corresponding weights and S.D. obtained over the 30 cells, are shown in the first line of Table 4. As can be seen, unlike with AO staining, only two decay components were observed with Rh123 staining: the longer component with 5.4 nsec having weight of 34% and the shorter component of 2.1 nsec with weight of 65% (for comparison, the FLT of Rh123 in water is about 4 nsec [31]). Following incubation with CCCP, FLT components were similarly shortened by 20%, yet their weight values were interchanged.

Measuring Rh123 FLT as a Function of Rh123 Concentration

The above experiments with Rh123-stained cells indicate that upon incubation with CCCP, intracellular

Table 4 FLT values measured in U937 cells stained with Rh123 treated with and without CCCP. The f is the weight of the decay component. Results are expressed as average of 30 cells ± STD. P< 0.001 vs control

Treatment	τ_1 [nsec]	f_1	τ_2 [nsec]	f_2
Control	5.39±0.58	0.34±0.03	2.08±0.04	0.65±0.04
CCCP	4.27±0.29	0.69±0.1	1.47±0.42	0.31±0.1

FLTs and corresponding weights undergo change. Based on other studies [15, 16], it is presumed that changes in the intracellular concentration of potentiometric probe such as Rh123, may be the result of CCCP treatment. This presumption is strengthened by the fact that Rh123 is not sensitive to micro environmental parameters such as pH and viscosity [32].

In order to directly examine the dependence of FLT upon Rh123 concentration, measurements of FLT of free cell Rh123 solutions were conducted. In order to minimize inner filtration influence upon FLT [33], front face fluorescence measurements were performed. In order to simulate the viscosity conditions that exist inside the cell, measurements were performed in viscous media (90% glycerol in PBS v/v) that are known to reduce the FLT from water media [18, 31]. The initial values of the FLT in these conditions are similar to the short component at the cells measurements. Results are given in Fig. 3.

Figure 3 shows that FLT is almost constant in up to 2 mM concentration of Rh123, and it decreases from 2 mM on. Results indicate that at 100 mM of Rh123, FLT is shorter than 1 nsec. These results, and additional data (not shown), indicate that dye concentration of Rh123 in the membrane, exceeds a few mM, and strengthen the suggested approach where FLT may be used for probing alteration in intracellular dye concentration caused by various physiological factors, one of which is changes in PMP.

Fluorescence Images of Rh123 Stained U937 Cells

Fluorescence images of Rh123 stained U937 cells, before and after incubation without and with 50 μM CCCP, were analyzed (Fig. 4). As can be seen in the cell image and from the curve describing the FI acquired along the profile line, the intensity distribution before treatment is much more heterogeneous than that of post-incubation with CCCP. This indeed confirms that CCCP causes the release of most, yet not all, of the intra organelle high density Rh123 into the cytoplasm. These findings are in agreement with the fact that two decay components were still found after CCCP treatment, where the shorter one is believed to indicate the existence of remaining Rh123 high concentration islets post-CCCP-treatment.

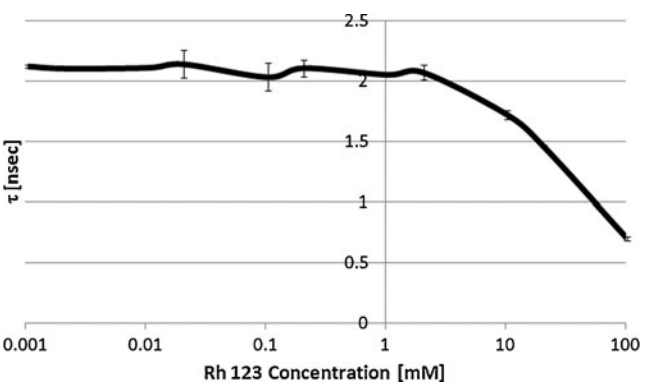

Fig. 3 FLT dependence upon Rh123 concentration in viscous media (90% glycerol in PBS v/v). $P<0.01$

Discussion and Conclusions

This study introduces a wo-FLT measurement approach for ease and a relatively economical option for tracing alterations in intracellular fluorophore distribution. It is a frequency domain based approach and its feasibility was examined using U937 cells stained with Rh123 and AO. The readout is the weights of the different emitters and their FLT as well. Correlating between simple FI images of a cell and its wo-FLT data may lead to the identification of the cellular sub-regions which are the sources for the wo-FLT data.

Examining Table 2 shows three decay components in AO stained untreated U937 cells. However, after treatment with apoptosis inducer H_2O_2, only two decay components were found. This strongly suggests that a significant cause for the measured changes in decay times, as well as the decay weights, is the alteration in intracellular fluorophore distribution. Therefore, tracing alterations in decay weights might gain insight into the quota of dye accumulated in the different intracellular regions, before and after treatment. FI color based image analysis, as well as spectra measurement cannot reveal such information, since even though the two emitter groups do not have the same FLT, they do have similar emission spectrum. For this reason, in such cases, wo-FLT measurements might be an ideal solution in order to investigate alteration in intracellular probe distribution in a "blind" manner. In cases where fluorophore distributions are indeed associated with changes in emission spectrum, FI color based image analysis is an obvious tool for investigation. Yet, it requires the use of quite cumbersome image analysis, which, in most cases, is subjective. On the other hand, using a black-white camera requires the use of color filters which compels consecutive measurements.

One potential application of the proposed wo-FLT approach is tracing alterations of membrane potential. The change of the decay component from 5.4 nsec to 4.27 nsec and corresponding weights from 34% to 79% following treatment with CCCP (Table 4), correlates with other findings which indicate that treatment with CCCP cause most of the mitochondrial Rh123 to leak into the cytoplasm in areas where the water phase is dominant [34]. While comparing the wo-FLT data to images of intensity (Fig. 4 upper panel),

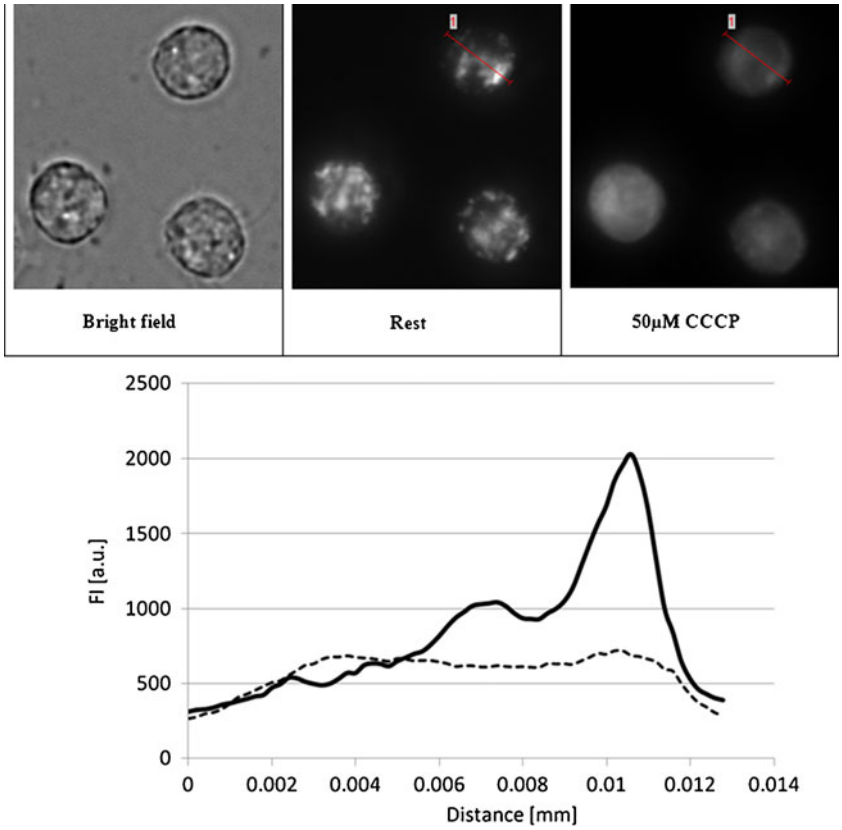

Fig. 4 The influence of CCCP treatment upon U937 cells. Measurements were performed on the same three cells which were stained with Rh123. *Upper panel*: transmitted light image (*left*) and fluorescence images of cells acquired after incubation without (*middle*) and with (*right*) 50 μM CCCP. *Lower panel*: The fluorescence intensity measured along the same profile line across the same cell (*right and upper*), after incubation without (*full line*) and with (*dashed line*) 50 μM CCCP. Ordinate: FI arbitrary units. Abscissa: distance (pixels) in mm

one can see that the dye is located in two regions only, and after treatment the dye becomes concentrated in one area only**.** This is strengthened by the fact that the FLT of Rh123 in aqua (PBS) is 4 nsec [31].

To the best of our knowledge, the wo-FLT approach has never been realized in cytometry. Moreover, the proposed wo-FLT method has a potential application in the detection of DNA hybridization with fluorescence label. When DNA is labeled with fluorophore in order to look for specific segment during hybridization, the intensity image remains identical, while only the FLT may change. In addition, the new method benefits biochemical experimentation with fluorescence label and is useful in cases where direct imaging is impossible**.** Moreover, in numerous cases where different sub-cellular stained regions share the same emission spectrum (e.g. U937 cells stained with either AO or Rh123) the wo-FLT approach is superior to that of color based FI image analysis in distinguishing between the different regions.

While dealing with advantages and disadvantages of the FLIM method, various implementations should be considered. In the use of wide-field FLIM (time-gated wide-field time domain as well as wide-field frequency domain) a serious problem exists with out-of-focus blur in the optical sectioning [35]. While using confocal or multi-photon scanning with TCSPC, acquiring time becomes very lengthy with each photon having to be timed individually. The wo-FLT method is not only virtually optically independent, fast, significantly less costly, simpler and easier to perform than the FLIM method, but may also address requirements which cannot be addressed via FLIM. For example, monitoring details of tumor growth, angiogenesis, and metastatic spread is almost impossible using direct imaging [36] or systems that involve compression of tissues by mechanical forces [37, 38]. In addition, bulk measurements with the FDTRM apparatus shown in Fig. 1 may support the wo-FLT method, but is not applicable with the FLIM method. The wo-FLT measurements are quite unique, not so much due to the technology used, but more for the fact that weights and decay times of several components are measured in a single cell resolution, skipping image analysis. The proposed approach suggests a new method within the field of single cell cytometry.

Acknowledgements This study was made possible through the Bequest of Moshe-Shimon and Judith Weisbrodt.

References

1. Shapiro HM (1995) Practical cytometry. Alan R. Liss Inc, New York, p 314, 315, and 327–329
2. Alberts B, Johnson A, Lewis J, Raff M, Roberts K, Walter P (2002) Molecular biology of the cell, 4th edition Chapter 9. Garland Science, New York

3. Birks JB (1970) Photophysics of aromatic molecules. Wiley, London
4. Cundall RB, Dale RE (1983) Time-resolved fluorescence spectroscopy in biochemistry and biology. Plenum, NATO ASI series. Series A, life sciences. New York
5. Valeur B (2002) Molecular fluorescence: principles and applications. Wiley–VCH, Weinheim
6. Miller JN (1981) Standard in fluorescence spectrometry. Chapman and Hall, London
7. Epps DE, Wolfe ML, Groppi V (1994) Characterization of the steady-state and dynamic fluorescence properties of the potential-sensitive dyes bis-(1,3- dibutylbarbituric acide) trimethine oxonol (Dibac4(3)) in model systems and cells. Chem Phys Lipids 69:137–150
8. Ando J, Smith NI, Fujita K, Kawata S (2009) Photogeneration of membrane potential hyperpolarization and depolarization in non-excitable cells. Eur Biophys J 38:255–262
9. Sorgenfrei S, Chiu C, Gonzalez RL Jr, Yu YJ, Kim P, Nuckolls C, Shepard KL (2011) Label-free single-molecule detection of DNA-hybridization kinetics with a carbon nanotube field-effect transistor. Nature Nanotechnology 6:126–132
10. Hsua YM, Chang CC (2009) A novel frequency method for quantitative analysis of fluorescence dye concentration by using series photodetector frequency circuit system. Sensor Actuator 154:23–29
11. Squire A, Verveer PJ, Bastiaens PI (2000) Multiple frequency fluorescence lifetime imaging microscopy. J Microsc 197:136
12. Kim DK, Cho ES, Um HD (2000) Caspase-dependent and independent events in apoptosis induced by hydrogen peroxide. Exp Cell Res 257:82–88
13. Stridh H, Kimland M, Jones DP, Orrenius S, Hampton MB (1998) Cytochrome c release and caspase activation in hydrogen peroxide and tributilin induced apoptosis. FEBS Lett 429:351–355
14. Zurgil N, Shafran Y, Fixler D, Deutsch M (2002) Analysis of early apoptotic events in individual cells utilizing fluorescence intensity and polarization measurements. Biochem Biophys Res Commun 290:1573–1582
15. Davis S, Weiss MJ, Wong JR, Lampidis TJ, Chen LB (1985) Mitochondrial and plasma membrane potentials cause unusual accumulation and retention of rhodamine 123 by human breast adenocarcinoma-derived MCF-7 cells. J Biol Chem 260:13844–13850
16. Baraccaa A, Sgarbib G, Solainib G, Lenaz G (2003) Rhodamine 123 as a probe of mitochondrial membrane potential: evaluation of proton flux through F0 during ATP synthesis. BBA - Bioenergetics 1606:137–146
17. Fixler D, Tirosh R, Deutsch M (2005) Tracing apoptosis and stimulation in individual cells by fluorescence intensity and anisotropy decay. J Biomed Opt 10:340071
18. Fixler D, Namer Y, Yishay Y, Deutsch M (2006) Influence of fluorescence anisotropy on fluorescence intensity and lifetime measurement: theory, simulations and experiments. IEEE Trans Biomed Eng 53:1141
19. Becker & Hickl GmbH, Modular FLIM Systems for Olympus Laser Scanning Microscope, Available from www.becker-hickl.com.
20. Robbins E, Marcus PI (1963) Dynamics of acridine orange–cell interaction, Interrelationships of acridine orange particles and cytoplasmic reddening. J Cell Biol 18:237–250
21. Paul BK, Samanta A, Guchhait N (2010) Implication toward a simple strategy to generate efficiency-tunable fluorescence resonance energy transfer emission: intertwining medium-polarity-sensitive intramolecular charge transfer emission to fluorescence resonance energy transfer. J Phys Chem A 114:6097–6102
22. Lamm ME, Neville DM Jr (1965) The dimer spectrum of acridine orange hydrochloride. J Phys Chem A 69:3872–3877
23. Shimosaka T, Sugii T, Hobo T, Ross JBA, Uchiyama K (2000) Monitoring of dye adsorption phenomena at a silica glass/water interface with total internal reflection coupled with a thermal lens effect. Anal Chem 72:3532–3538
24. Zelenin AV (1966) Fluorescence microscopy of lysosomes and related structures in living cells. Nature 212:425–426
25. Antunes F, Cadenas E, Brunk UT (2001) Apoptosis induced by exposure to a low steady-state concentration of H2O2 is a consequence of lysosomal rupture. Biochem J 356:549–555
26. Ito F, Kakiuchi T, Nagamura T (2007) Excitation energy migration of acridine orange intercalated into deoxyribonucleic acid thin films. J Phys Chem C 111:6983–6988
27. Tomita G (1967) Fluorescence-excitation spectra of acridine orange-DNA and -RNA systems. Biophysik 4:23
28. Belyaeva TN, Krolenko SA, Leontieva EA, Mozhenok TP, Salova AV, Faddeeva MD (2009) Acridine orange distribution and fluorescence spectra in myoblasts and single muscle fibers. Cell and Tissue Biol 3:173–180
29. Zelenin AV ((1999)) Acridine orange as a probe for cell and molecular biology, in fluorescent and luminescent probes for biological activity. Elsevier
30. Kapuscinski J, Darzynkiewicz Z (1987) Interactions of acridine orange with double stranded nucleic acids. Spectral and affinity studies. J Biomol Struct Dyn 5:127–143
31. Eggeling C, Berger S, Brand L, Fries JR, Schaffer J, Volkmer A, Seidel CAM (2001) Data registration and selective single-molecule analysis using multi-parameter fluorescence detection. J Biotechnol 86:163–180
32. Deumié M, Lorente P, Morizon D (1995) Quantitative binding and aggregation of R123 and R6G rhodamines at the surface of DPPG and DPPS phospholipid vesicles. J Photochem Photobiol Chem 89:239–245
33. Hu C, Muller-Karger FE, Zepp RG (2002) Absorbance, absorption coefficient, and apparent quantum yield: a comment on common ambiguity in the use of these optical concepts. Limnol Oceanogr 47:1261
34. Johnson LV, Walsh ML, Bockus BJ, Chen LB (1981) Monitoring of relative mitochondrial membrane potential in living cells by fluorescence microscopy. J Cell Biol 88:526–535
35. Cole MJ, Siegel J, Webb SED, Jones R, Dowling K, French PMW, Lever MJ, Sucharov LOD, Neil MAA, Juskaitis J, Wilson T (2000) Whole-field optically sectioned fluorescence lifetime imaging. Opt Lett 25:1361–1363
36. Yang M, Baranov E, Wang JW, Jiang P, Wang X, Sun FX, Bouvet M, Moossa AR, Penman S, Hoffman RM (2002) Direct external imaging of nascent cancer, tumor progression, angiogenesis, and metastasis on internal organs in the fluorescent orthotopic model. Proc Natl Acad Sci USA 99:3824–3829
37. Grodzinsky AJ, Levenston ME, Jin M, Frank EH (2002) Cartilage tissue remodeling in response to mechanical forces. Annu Rev Biomed Eng 2:691–713
38. Wang PY, Chow HH, Lai JY, Liu HL, Tsai WB (2009) Dynamic compression modulates chondrocyte proliferation and matrix biosynthesis in chitosan/gelatin scaffolds. J Biomed Mater Res B Appl Biomater 91B:143–152